Rosmarinic Acid Analogue-11 Induces Apoptosis of Human Gastric Cancer SGC-7901 Cells via the Epidermal Growth Factor Receptor (EGFR)/Akt/Nuclear Factor kappa B (NF-κB) Pathway

Authors' Contribution:
Study Design A
Data Collection B
Statistical Analysis C
Data Interpretation D
Manuscript Preparation E
Literature Search F
Funds Collection G

BCEF 1 **Wanting Li**
AB 2 **Qing Li**
AD 1 **Liqun Wei**
BC 3 **Xiaohang Pan**
AF 1 **Daohang Huang**
DG 3 **Jialiang Gan**
AG 1 **Shuangyi Tang**

1 Department of Pharmacy, The First Affiliated Hospital of Guangxi Medical University, Nanning, Guangxi, P.R. China
2 College of Pharmacy, Guangxi Medical University, Nanning, Guangxi, P.R. China
3 Department of Colorectal Anal Surgery, The First Affiliated Hospital of Guangxi Medical University, Nanning, Guangxi, P.R. China

Background: According to the latest statistics from the American Cancer Society, there will be 1.73 million cancer cases and more than 600 000 cancer deaths in the United States in 2018, among which there will be 26 240 new cases of gastric cancer and around 10 800 deaths arising from gastric cancer. The objective of this study was to use RAA-11 to intervene in SGC-7901 cells to understand its effects on cell proliferation and apoptosis, and to explore the apoptosis mechanism.

Material/Methods: MTT assay was used to detect the survival of human gastric mucosal epithelial GES-1 cells and human gastric cancer SGC-7901 cells. Colony formation assay was used to observe the colony forming ability in SGC-7901 cells. The apoptotic rate of SGC-7901 cells was evaluated by Hoechst33258 staining and flow cytometry. qRT-PCR was used to analyze the epidermal growth factor receptor (EGFR) mRNA expression level in SGC-7901 cells. Western blot was used to examine the expression levels of caspase-3, Bcl-2, BAX, EGFR, Akt, p-Akt, and NF-κB in SGC-7901 cells.

Results: RAA-11 is capable of inhibiting the proliferation and inducing the apoptosis of SGC-7901 cells in a time- and dose-dependent manner. Western blot showed that the expression levels of caspase-3 and BAX were upregulated, while the expression levels of Bcl-2, EGFR, Akt, p-Akt, and NF-κB in the SGC-7901 cells were downregulated.

Conclusions: Apoptosis can be induced in SGC-7901 cells by RAA-11, potentially via the EGFR/Akt/NF-κB pathway, indicating that RAA-11 might be a potent agent for cancer treatment.

MeSH Keywords: Apoptosis • Cell Proliferation • Genes, erbB-1 • NF-kappa B • Proto-Oncogene Proteins c-akt • Rosmarinus

Full-text PDF: https://www.basic.medscimonit.com/abstract/index/idArt/913331

📄 3594   ▥ 6   📊 9   📖 48

Background

Cancer is a major public health problem worldwide and the second leading cause of death in humans [1]. According to the latest statistics from the American Cancer Society, there will be 1.73 million cancer cases and more than 600 000 cancer deaths in the United States in 2018, among which there will be 26 240 new cases of gastric cancer and around 10 800 deaths arising from gastric cancer [2]. As such, gastric cancer should be considered a worldwide public health problem [3]. Surgery and chemotherapy are the main treatment methods for gastric cancer, and have been effective in reducing mortality, but the 5-year survival rate of gastric cancer patients is still relatively low [4]. Nowadays, various new natural compounds, such as podophyllin, paclitaxel, camptothecin, and vinblastine, have been isolated and used as effective drugs for cancer treatment, but their side effects are relatively large [5]. So, finding a new drug to treat stomach cancer is crucial [6]. Rosmarinic acid (RA) is a type of natural phenol carboxylic acid, which is a secondary metabolite commonly used in cooking herbs and commonly found in herbs such as rosemary, sage, thyme, and mint [7]. RA has a variety of promising biological effects, including anti-cancer [8], anti-microbial [9], anti-anaphylaxis, anti-inflammatory [10], and antioxidant [11]. For instance, Rocha et al. identified the anti-inflammatory potential of RA in rat models of local and systemic inflammation for the first time [10]. Han et al. found that RA might potentially be a therapeutic agent for suppressing the Warburg effect in gastric carcinoma [8]. Hence our research group synthesized a dozen RA analogues (RAAs). The preliminary experiment found that RAA-11 had the most prominent anti-cancer effect, with a molecular weight of 377.34. Its molecular structure formula and synthesis route are shown in Figure 1. Its MS and ^{1}H-NMR are shown in Figures 2 and 3 respectively. Therefore, this study applied RAA-11 to intervene on human gastric cancer SGC-7901 cells to understand its effects on cell proliferation and apoptosis, and explore their apoptosis mechanism so as to provide fundamental theories for further research.

Material and Methods

Main reagents and preparation

RAA-11 was synthesized from the College of Pharmacy, Guangxi Medical University, with a purity of 98% or more. Brief synthetic steps are described as follows: 1.21 g methyl ester hydrochloride was dissolved in 5 mL DMF and stirred at 0–5°C for 10 minutes. Then the solution had added, drop wise, 0.75 g of 3, 4-difluorocinnamic acid dissolved in 10 mL dichloromethane solution as well as 2.12 g PyBOP and 1.63 mL triethanolamine. After reaction for 30 minutes, the mixture was stirred for 16 hours at room temperature and then extracted with ethyl acetate, then successively washed with 1 M hydrochloric acid solution, 10% sodium bicarbonate solution, water, and saturated sodium chloride solution. Then the solution was dried with anhydrous sodium sulphate to harvest a 1.32 g flavescent oily substance (RAA-11). RAA-11 was dissolved in DMSO to make into 50 mmol/L stock solution, and preserved at −20°C away from sunlight. During the experiment, RAA-11 stock solution was diluted to high, medium, and low concentration (40 µmol/L, 20 µmol/L, and 10 µmol/L respectively) with the Roswell Park Memorial Institute-1640 (RPMI-1640) Medium supplemented with 10% fetal bovine serum (FBS), 100 µg/mL streptomycin, and 100 U/mL penicillin. Annexin V-FITC/PI Apoptosis Detection Kit was purchased from Becton, Dickinson and Company (New York, NY, USA). AxyPrep™ Multisource Total RNA Miniprep Kit was purchased
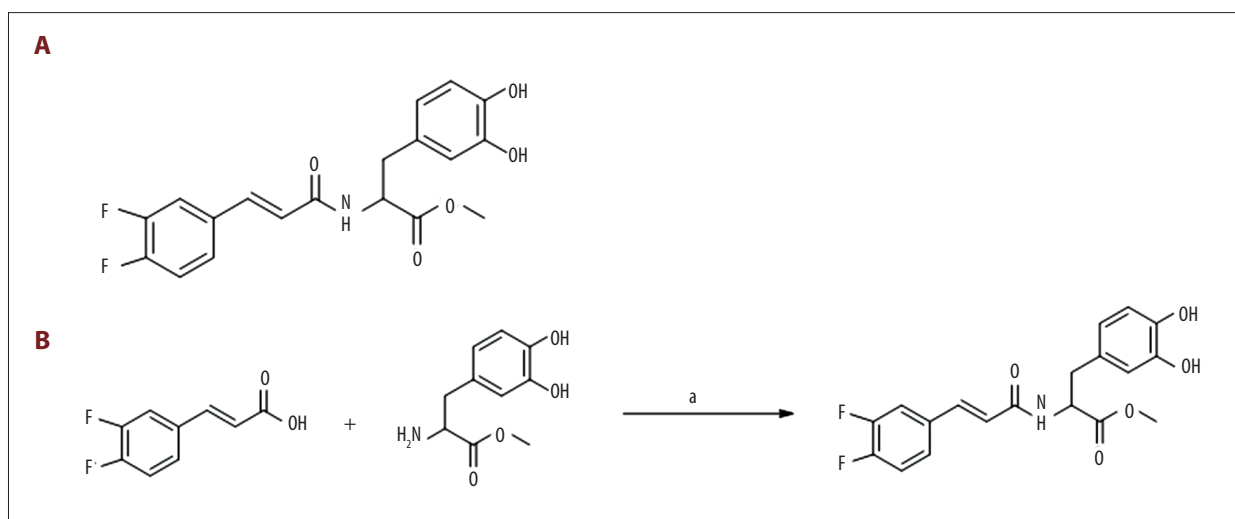

Figure 1. Molecular structure and synthetic route schematic of RAA-11. (**A**) Molecular structure of RAA-11. (**B**) Synthetic route schematic of RAA-11. a – PyBOP, TEOA, DMF, DCM.
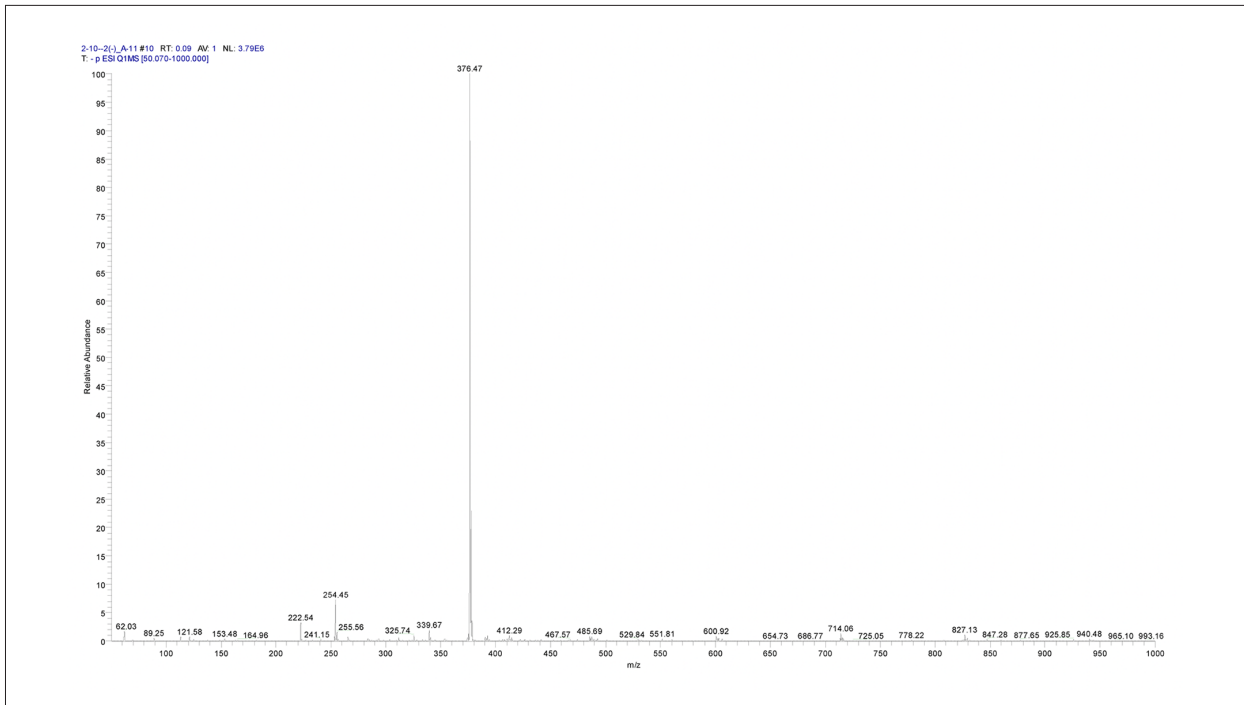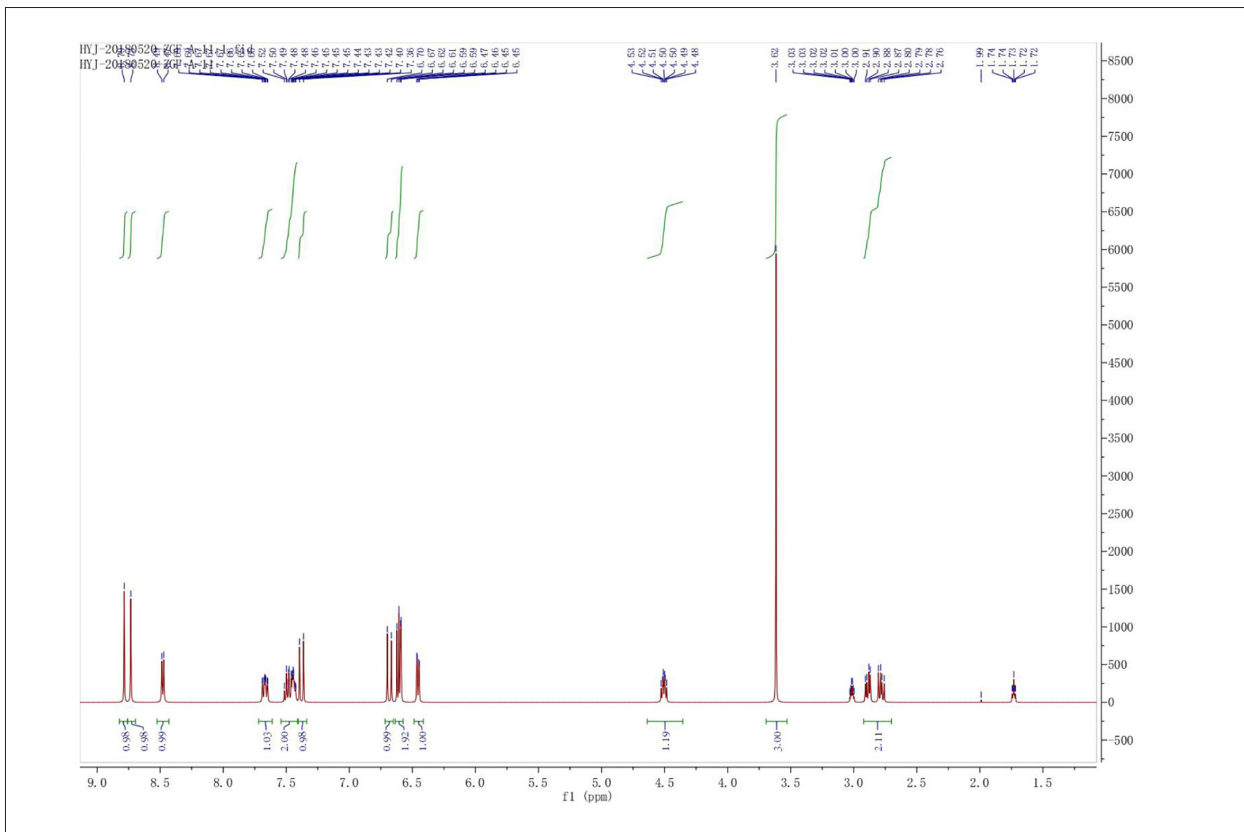
Figure 2. MS of RAA-11.

Figure 3. ¹H-NMR of RAA-11 (¹H NMR (500 MHz, DMSO-d_6) δ 8.79 (s, 1H), 8.73 (s, 1H), 8.48 (d, J=7.7 Hz, 1H), 7.67 (m, J=11.9, 7.9, 2.0 Hz, 1H), 7.54–7.41 (m, 2H), 7.38 (d, J=15.8 Hz, 1H), 6.68 (d, J=15.8 Hz, 1H), 6.64–6.57 (m, 2H), 6.46 (dd, J=8.0, 2.1 Hz, 1H), 4.64–4.36 (m, 1H), 3.62 (s, 3H), 2.92–2.70 (m, 2H).

from Axygen BioScience, Inc. (United City, CA, USA). RevertAid First Strand cDNA Synthesis Kit was purchased from Thermo Fisher Scientific Inc. (Shanghai, China). SYBR® Premix Ex Taq™ II (Tli RNaseH Plus) was purchased from Takara Biomedical Technology Co., Ltd. (Beijing, China). Epidermal growth factor receptor (EGFR) mRNA and GAPDH mRNA were purchased from GenScript Biotech Corp. Co., Ltd. (Nanjing, Jiangsu, China). EGFR, Akt, p-Akt, NF-κB, GAPDH, BAX, Bcl-2, and caspase-3 rabbit anti-human monoclonal antibodies were purchased from Wanleibio Co., Ltd. (Shenyang, Liaoning, China). Dylight 680 AffiniPure Goat Anti-Rabbit IgG (H+L) was purchased from EarthOx, LLC (San Francisco, CA, USA).

Apparatus

The inverted fluorescence microscope was purchased from Nikon Corporation (Tokyo, Japan). The BX53 positive fluorescence microscope was purchased from Olympus Corporation (Tokyo, Japan). ELx800 microplate reader was purchased from BioTek Inc. (VT, USA). Flow Cytometry was purchased from Becton, Dickinson and Company (New York, NY, USA). NanoDrop 2000 Spectrophotometer was purchased from Thermo Fisher Scientific Inc. (Shanghai, China). StepOnePlus™ Real-Time PCR System was purchased from Thermo Fisher Scientific Inc. (Shanghai, China). SDS-PAGE electrophoresis meter and Trans-Blot SD were purchased from Bio-Rad (Hercules, CA, USA). LI-COR Odyssey 2-tone infrared fluorescence imaging system was purchased from LI-COR Biosciences Inc. (Lincoln, NE, USA).

Cell culture

Human gastric mucosal epithelial cell lines GES-1 and human gastric cancer cell lines SGC-7901 were obtained from the Shanghai Cell Bank, Chinese Academy of Sciences (Shanghai, China). The cells were routinely cultured in RPMI-1640 medium with 10% FBS and 100 μg/mL streptomycin, and 100 U/mL penicillin in the 37°C in a 5% CO_2 incubator. When the cells grew exponentially, they were digested with trypsin.

3-(4,5-dimethyl-2-thiazolyl)-2,5-diphenyl- 2-H-tetrazolium bromide (MTT) assay

The MTT (3-(4,5-dimethyl-2-thiazolyl)-2,5-diphenyl-2-H-tetrazolium bromide) assay was performed as described previously [12]. Human gastric mucosal epithelial GES-1 cells and human gastric cancer SGC-7901 cells were routinely cultured and digested at exponential phase. The cells were diluted into a concentration of $5×10^4$ cells/mL by RPMI-1640 medium containing 10% FBS and inoculated into 96-well plates with 100 μL per well. The culture solution was discarded after the cells adhered to the wall. Then, 200 μL of RAA-11 with 0, 10, 20, 40, 80, and 160 μmol/L was added to each well, and 5 duplicate wells were set for each dose group. After the cells were cultured for

24 hours, 36 hours, and 48 hours, 20 μL of 5 mg/mL MTT was added per well and cultured for 4 hours in a 37°C incubator. Then each well had added 100 μL DMSO for 10 minutes. The optical density (OD) value of the each well was determined using the 570 nm microplate reader to calculate cell survival.

Colony formation assay

Colon formation assay was performed as described previously [13]. When the human gastric cancer SGC-7901 cells were digested at exponential phase, the cell suspension was diluted to $1×10^3$ cells/mL. After manipulating them to single cell suspension, 500 μL cell suspension per well were placed in a 6-well plate with 1 mL RPMI-1640 medium containing 10% FBS. Then 2 mL of RAA-11 (0, 10, 20, and 40 μmol/L) were added to each well after the cells adhered to the wall, and the RPMI-1640 medium was replaced on alternate days to make the cells grow for 1 to 2 weeks (when the colony was visible to the naked eye). The cells were washed 2 times with phosphate buffer saline (PBS), and fixed in 4% paraformaldehyde fix solution for 15 minutes after air-dried at room temperature. Then the cells were dyed for 20 minutes with 1% crystal violet staining solution. Images were taken under the inverted fluorescence microscope to count the Colony Forming Unit (CFU).

Hoechst33258 stain assay

The Hoechst33258 stain assay was performed as described previously [14]. When the human gastric cancer SGC-7901 cells were digested at exponential phase, the cell suspension was diluted to $2×10^4$ cells/mL. Then 2 mL of cell suspension were inoculated into a 6-well plate with embedded with aseptically treated cover glass. Then 2 mL of RAA-11 (0, 10, 20, and 40 μmol/L) were added to each well after the cells adhered to the wall. After 48 hours, the cells were washed with PBS twice, and fixed with 1 mL of 4% paraformaldehyde fix solution at room temperature for 20 minutes. Then, the cells were stained with 500 μL Hoechst33258 stain solution at room temperature away from light for 15 minutes. Finally, the cells were gently rinsed twice with PBS. The cover glass was placed on the clean microslides and sealed with a drop of Antifade Mounting Medium. The fluorescence intensity of the Hoechst33258 was observed using BX53 positive fluorescence microscopy.

Flow cytometry

Flow cytometry was performed as described previously [14]. When the human gastric cancer SGC-7901 cells were digested at exponential phase, the cell suspension was diluted to $1.5×10^5$ cells/mL and 2 mL of the cell suspension were inoculated into a 6-well plate. Then 2 mL of RAA-11 (0, 10, 20, and 40 μmol/L) were added to each well after the cells adhered to

Table 1. First strand cDNA synthesis.

Total RNA	1 µg
Oligo (dT)$_{18}$ primer	1 µL
Water, nuclease-free	to 12 µL
5× reaction buffer	4 µL
RiboLock RNase Inhibitor (20 U/µL)	1 µL
10 mM dNTP Mix	2 µL
RevertAid M-MuLV RT (200 U/µL)	1 µL
Total volume	20 µL

Table 2. Primer sequences and length of amplification products of GAPDH and EGFR.

Gene name		Primer sequence (5'-3')
GAPDH	Forward	5'-GTCTTCACCACCATGGAGAAG-3'
	Reverse	5'-GTTGTCATGGATGACCTTGGC-3'
EGFR	Forward	5'-CCTGGTCTGGAAGTACGCAG-3'
	Reverse	5'-CGATGGACGGGATCTTAGGC-3'

Table 3. PCR solution components.

SYBR® Premix Ex TaqII (Tli RNaseH Plus) (2×)	10 µL
PCR forward primer (10 µM)	0.8 µL
PCR reverse primer (10 µM)	0.8 µL
ROX reference dye (50×)	0.4 µL
cDNA	2 µL
Water, nuclease-free	6 µL
Total volume	20 µL

the wall. After 48 hours, the supernatant and cells were centrifuged for 5 minutes at 1000 rpm. Then 1 mL iced PBS was added to resuspend the cells, and centrifuged for 5 minutes at 1000 rpm.200 µL 1×Binding Buffer was added to resuspend cells, followed by 5 µL propidium iodide (PI) and 5 µL Annexin V-FITC to incubate for 15 minutes at room temperature. Then 300 µL 1x Binding Buffer was added. The cell suspension was filtered through 300 mesh filter once and tested within 1 hour.

Quantitative real-time PCR

Quantitative real-time PCR (qRT-PCR) was performed as described previously [15]. When the human gastric cancer SGC-7901 cells were digested at exponential phase, they were cultured in 25 cm^2 culture bottles for 24 hours and treated with 3 mL of RAA-11 with final concentration at 0, 10, 20, and 40 µmol/L respectively. After 48 hours, the supernatant and cells were collected, and centrifuged for 5 minutes at 2000 rpm. Then 400 µL Buffer R-I was added to resuspend the cells and then transferred to a 1.5 mL centrifuge tube. 150 µL Buffer R-II was added in the 1.5 mL centrifuge tube, followed by centrifuge for 5 minutes at 12 000 rpm at 4°C. The supernatant fluid was transferred into a 1.5 mL centrifugal tube, and 250 µL of 2-propanol was added to the tube and the mixture was mixed evenly. The mixture was put in a 2 mL centrifuge tube and centrifuged for 1 minute at 6000 rpm at 4°C. The filtrate was then discarded. We added 500 µL Buffer W1A and centrifuged for 1 minute at 12 000 rpm. The filtrate was then discarded once more and 700 µL Buffer W2 was added and centrifuged for 1 minute at 12 000 rpm. The last process was repeated once more. The preparation tube was put into a new 1.5 mL centrifuge tube and 30 µL Buffer TE was added in the preparation tube. Finally, the cells were centrifuged for 1 minute at 12 000 rpm and eluted to get RNA. The NanoDrop 2000 Spectrophotometer was used to detect the RNA concentration, after which the RNA was put at −80°C for storage. Reverse transcription was performed on ice according to kit instruction, and the reaction system of each sample is shown in Table 1. The First Strand cDNA Synthesis was mixed gently and centrifuged briefly, then incubated for 60 minutes at 42°C

and the reaction was terminated by heating at 70°C for 5 minutes. The cDNA can be stored at −20°C for less than 1 week.

Based on the gene sequences of human GAPDH and EGFR in the NCBI Gene Bank, the primers were designed and synthesized by GenScript Biotech Corp., Co., Ltd., with the sequences shown in Table 2.

PCR amplification was performed on ice according to kit instruction, and the reaction system of each sample is shown in Table 3.

The data was analyzed by a relatively quantitative analysis. The $2^{-\Delta\Delta Ct}$ values were calculated to compare the level of gene expression in various groups. All values were normalized against GAPDH values.

Western blot

Western blot was performed as previously described [12]. When the human gastric cancer SGC-7901 cells were digested at exponential phase, they were cultured in 25 cm^2 culture bottles for 24 hours and treated with 3 mL of RAA-11 with final concentration at 0, 10, 20, and 40 µmol/L respectively. After 48 hours, the supernatant and cells were collected and washed with PBS 3 times. The cells were lysed on ice for 20 minutes with Lysis Buffer (RIPA: PMSF: Cocktail=100: 1: 1), centrifuged for 20 minutes at 12 000 rpm at 4°C. After which BCA Protein Assay was used to detect protein concentration, the supernatant was

Table 4. Influence of RAA-11 on the survival rate of human gastric mucosa epithelial cells GES-1 at different concentrations at different times ($\overline{\chi}\pm S$, n=3).

Concentration/µmol/L	Cell survival rate%		
	24 h	36 h	48 h
0	100.000±0.000	100.000±0.000	100.000±0.000
10	91.587±1.459***	88.050±2.225***	84.002±1.200***
20	83.673±1.750***	81.593±1.966***	78.757±1.533***
40	77.053±2.488***	74.313±0.704***	71.110±1.199***
80	71.173±0.729***	67.693±1.168***	65.520±0.824***
160	66.313±1.791***	58.247±1.596***	56.267±0.860***

*** $P<0.001$ versus 0 µmol/L group at the same time.

Table 5. Influence of RAA-11 on the survival rate of human gastric cancer cells SGC-7901 at different concentrations at different times ($\overline{\chi}\pm S$, n=3).

Concentration/µmol/L	Cell survival rate%		
	24 h	36 h	48 h
0	100.000±0.000	100.000±0.000	100.000±0.000
10	87.263±0.992***	81.147±0.984***	73.193±0.729***
20	79.023±1.753***	76.007±1.909***	66.620±1.502***
40	59.123±1.527***	54.963±2.001***	43.160±1.040***
80	46.657±1.163***	41.227±1.373***	26.037±1.768***
160	23.333±2.082***	20.983±0.715***	15.343±0.890***

*** $P<0.001$ versus 0 µmol/L group at the same time.

Table 6. IC_{50} of RAA-11 on GES-1 and SGC-7901 cells at different times.

Cell strains	IC_{50} (µmol/L)		
	24 h	36 h	48 h
GES-1	289.425±0.854	220.430±2.300	189.521±1.002
SGC-7901	73.299±2.011	50.426±1.458	37.684±0.579

boiled with SDS-PAGE Sample Loading Buffer for 5 minutes. Then 40 µg samples of protein were separated by electrophoresis at 60V constant pressure. When the samples reached the separation gel, the voltage was changed to 120V until samples reached the bottom of the gel. Trans-Blot SD was used to transfer the protein onto the polyvinylidene difluoride (PVDF) membranes. The PVDF membranes were washed 3 times with TBST and sealed with 5% BSA at room temperature for 30 minutes. Next, the PVDF membranes were washed 3 times with TBST and incubated with rabbit anti-human monoclonal antibodies overnight at 4°C and then incubated with Dylight 680 AffiniPure Goat Anti-Rabbit IgG (H+L) under the conditions of protection from light at room temperature for 1 hour. After the PVDF membranes were washed 3 times with TBST away from light, the films were scanned on Odyssey Infrared Imaging System. All values were normalized against GAPDH values.

Statistical analysis

SPSS20.0 statistics software (SPSS Inc., USA) was used to carry out the statistical analysis, measured values were expressed with mean ± standard deviation ($\overline{\chi}\pm S$), The t-test was used for the comparison between groups, single factor analysis of variance was used when there was comparison of more than 2 groups. Bilateral test was selected. $P<0.05$ value was considered as statistically significant and all techniques were replicated 3 times.
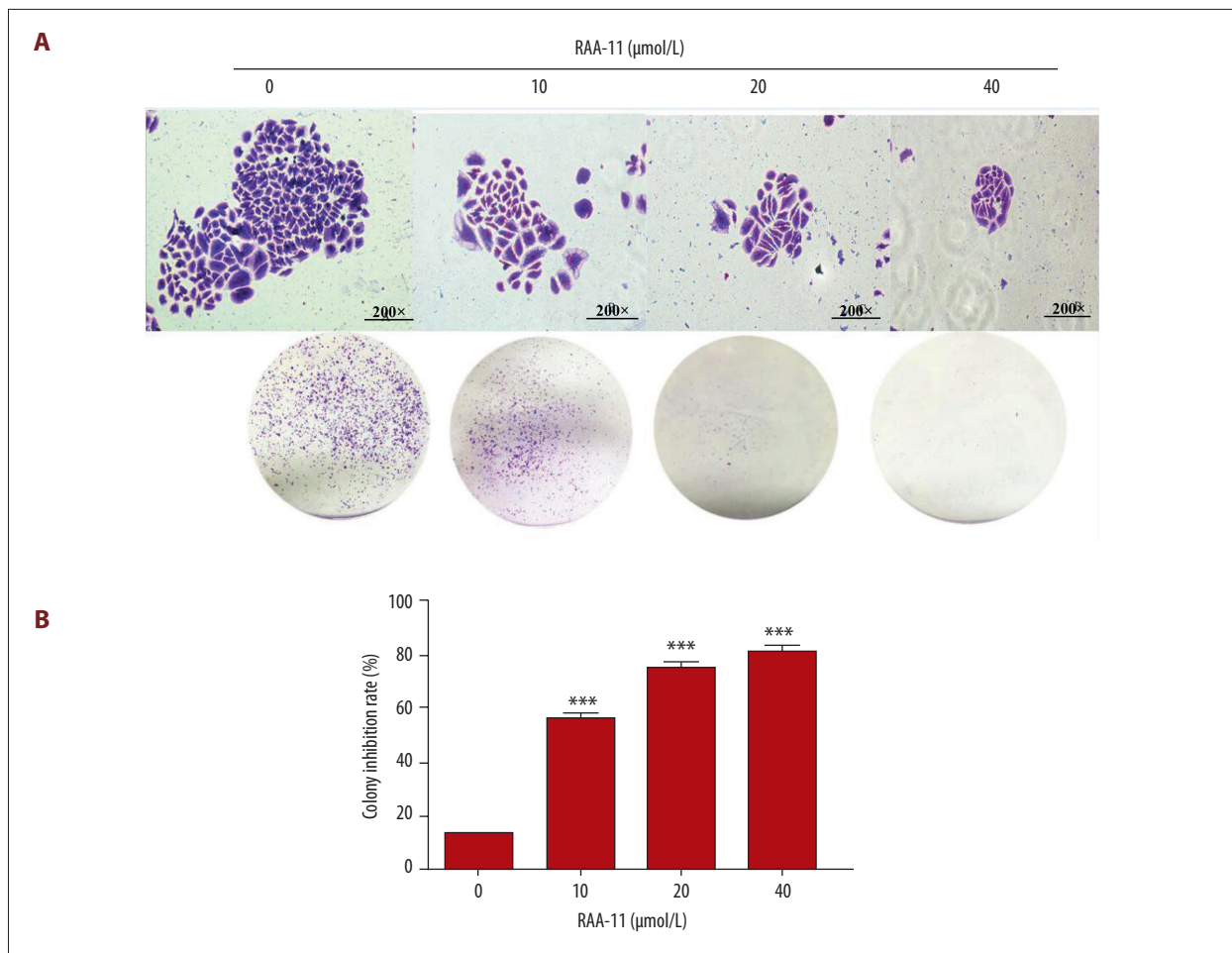
Figure 4. Colony formation assay results. (**A**) Influence of different concentrations of RAA-11 on colony forming ability of Human gastric cancer cells SGC-7901. (**B**) Histogram of colony inhibition rate. ($\overline{\chi}\pm S$, n=3), *** P<0.001 versus 0 µmol/L group.

Results

Evaluation of survival rate by using MTT assay

As shown in Tables 4 and 5, the basal proliferation rate of SGC-7901 cells exhibited statistically significant differences compared with GES-1 cells. The inhibitory effect on the proliferation of SGC-7901 cells increased in a time- and concentration-dependent manner. Table 6 shows that the IC_{50} of RAA-11 at 24 hours, 36 hours, and 48 hours on GES-1 cells was 289.425±0.854 µmol/L, 220.430±2.300 µmol/L, and 189.521±1.002 µmol/L respectively, whereas the IC_{50} of RAA-11 at 24 hours, 36 hours, and 48 hours of SGC-7901 cells was 73.299±2.011 µmol/L, 50.426±1.458 µmol/L, and 37.684±0.579 µmol/L respectively.

Evaluation of cell colony formation ability by using colony formation assay

As shown in Figure 4, compared to the 0 µmol/L group (P<0.001), the colony inhibition rate of SGC-7901 cells increased in a concentration-dependent manner. The colony inhibition rates of RAA-11 at 0 µmol/L, 10 µmol/L, 20 µmol/L, and 40 µmol/L were 12.68%, 56.48%, 75.64%, and 83.66% (colony inhibition rate (%)=($CFU_{control group}$−$CFU_{dose group}$)/$CFU_{control group}$×100%).

Evaluation of morphological changes of apoptosis by using Hoechst33258 stain assay

Hoechst33258 assay combines with nuclear condensation and fragmentation in the apoptotic cells, showing a strongly fluorescent reaction. The viable non-apoptotic cells do not undergo pyknotic nucleus or rhexes but show relatively light fluorescence. As shown in Figure 5, compared to the 0 µmol/L group (P<0.001), the SGC-7901 cells showed obvious apoptosis after treatment with RAA-11 for 48 hours, and the cell apoptotic rate (cell apoptotic rate(%)=apoptotic cellular score/total cellular score×100%) increased significantly in a dose-dependent manner.
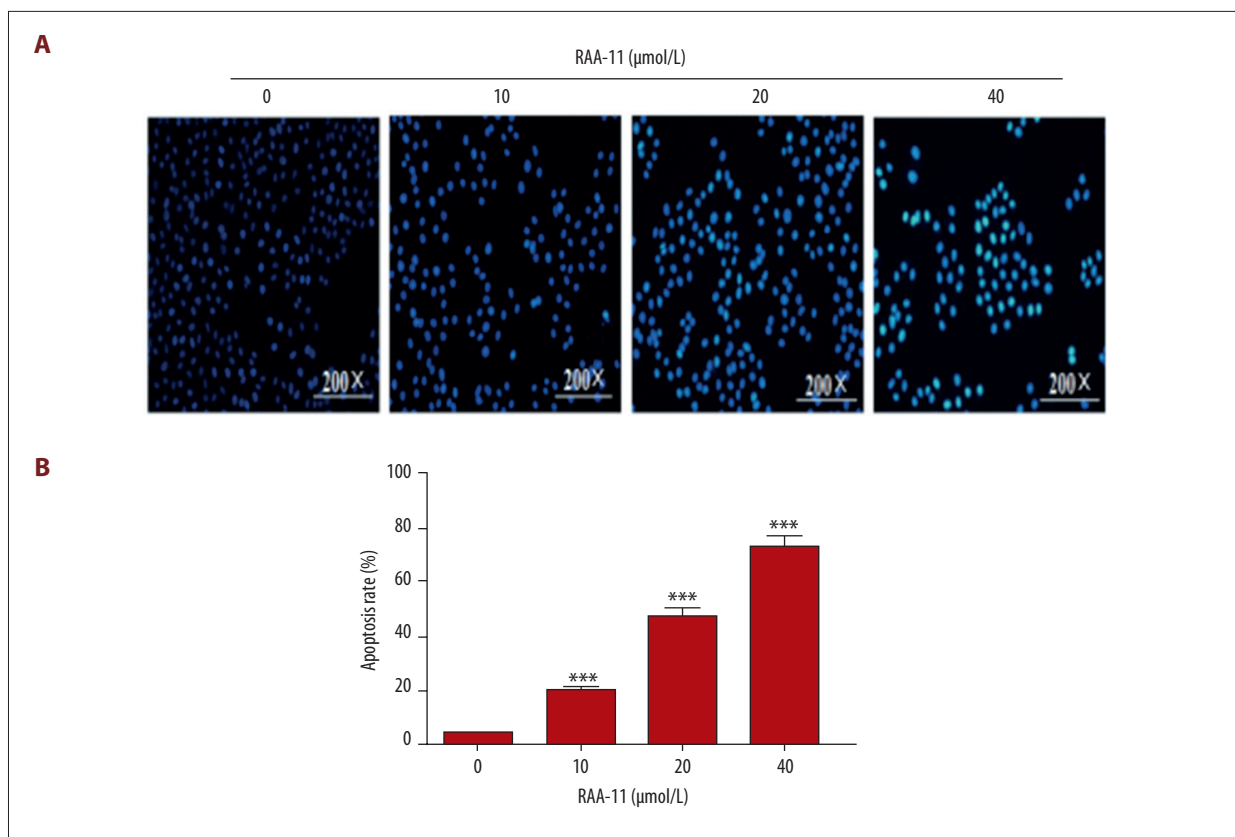
Figure 5. Hoechst33258 stain assay results. (**A**) Influence of different concentrations of RAA-11 on apoptotic nucleus of Human gastric cancer cells SGC-7901. (**B**) Histogram of apoptotic rate. ($\overline{\chi}\pm$S, n=3), *** $P<0.001$ versus 0 µmol/L group.

Evaluation of apoptosis rate by using flow cytometry

The effects of RAA-11 on apoptosis include early apoptosis (Annexin V+/PI–) and late apoptosis (Annexin V+/PI+). As shown in Figure 6, the apoptotic rate was 4.09% (0 µmol/L), 39.77% (10 µmol/L), 42.72% (20 µmol/L), and 51.12% (40 µmol/L), respectively. The data exhibited RAA-11 could induce apoptosis of SGC-7901 cells in a dose-dependent manner ($P<0.001$).

Evaluation of expression level of EGFR mRNA by using qRT-PCR

As shown in Figure 7, the expression level of EGFR mRNA was significantly downregulated compared to the 0 µmol/L group ($P<0.001$), indicating that RAA-11 can downregulate the mRNA expression level of the EGFR gene in SGC-7901 cells.

Evaluation of expression level of relative proteins by using western blot

As shown in Figures 8 and 9, the expression of inhibitory apoptotic protein Bcl-2 was decreased and the expression of pro-apoptotic protein BAX and caspase-3 was increased when compared with the 0 µmol/L group ($P<0.001$). The expression

of pathway proteins EGFR, Akt, p-Akt, and NF-κB was significantly downregulated ($P<0.001$), suggesting that RAA-11 may induce apoptosis of SGC-7901 cells by inhibiting the EGFR/Akt/NF-κB pathway.

Discussion

Rosemarinic acid (RA) is a kind of polyphenols hydroxyl compound [16]. It contains a molecule of caffeic acid and a molecule of 3,4-dihydroxy phenyl lactic acid [17]. In recent years, more and more attention has been paid to rosemary, with numerous reports on the chemical composition and pharmacological effects of rosemary [18]. Nowadays, the treatment of malignant tumors has become a major difficulty that we urgently need to overcome. RA is rich in a variety of plants, and it can play an anti-tumor role through a variety of ways and also has a good application prospect as an anti-tumor drug [19].

In contrast to necrosis, apoptosis is the most common form of cellular physiological death (non-pathological cell death) [20], which can occur in various stages of embryonic development, tissue reconstruction, immunoregulation, and tumor regression [21]. Caspase-3 is a protease containing 277 amino acid
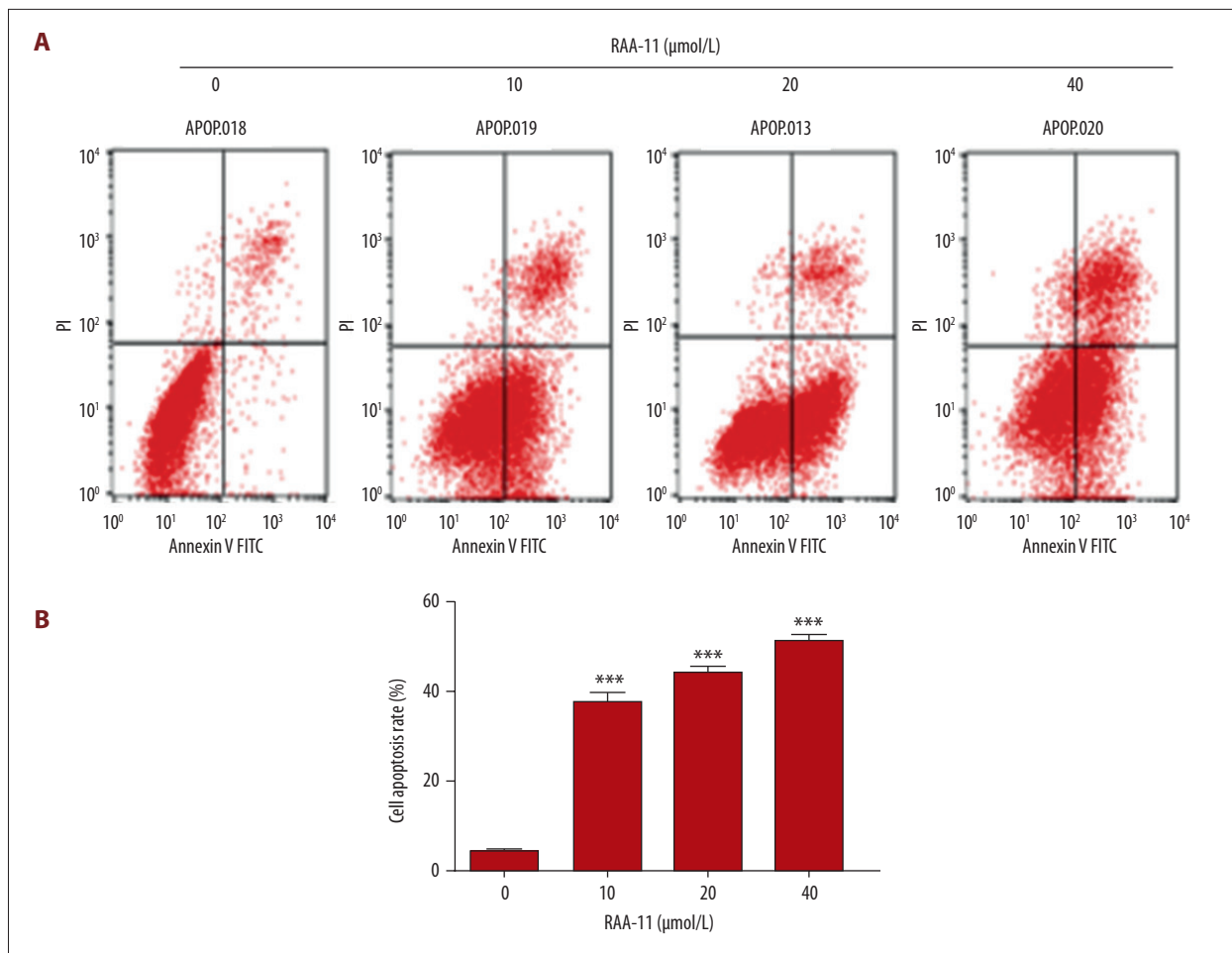
Figure 6. Flow cytometry results. (**A**) Influence of different concentrations of RAA-11 on apoptotic rate of Human gastric cancer cells SGC-7901. (**B**) Histogram of cell apoptotic rate. ($\bar{\chi}$±S, n=3), *** P<0.001 versus 0 µmol/L group.

residues, with a molecular weight of about 32 kDa [22], and it is one of the most important terminal shear enzyme of the caspase family in cell apoptosis [23]. Its downstream factor, Bcl-2, is an oncogene that inhibits apoptosis. Currently, the Bcl-2 protein family can be divided into 2 types according to function [24]. One type, similar to Bcl-2, can inhibit apoptosis such as Bcl-XL, Bcl-W, Mcl-1, and A1. While the other type can promote apoptosis, such as BAX, Bcl-Xs, Bik/Nbk, and Bid [25]. Our research showed that RAA-11 can promote the expression of apoptotic initiator caspase-3 and pro-apoptotic factor BAX, and inhibit the expression of apoptosis factor Bcl-2. Therefore, we deem that RAA-11 can induce the apoptosis of human gastric cancer SGC-7901 cells.

In tumor cells, EGFR promotes growth by promoting the proliferation and inhibiting the apoptosis of tumor cells [26]. Furthermore, numerous studies exhibited that EGFR is closely related to inflammation. Mu et al. found that epidermal growth factor receptor 2 (HER2) overexpression was observed at a higher rate in inflammatory breast cancer compared with

noninflammatory breast cancer [27]. Li et al. report on *in vitro* and *in vivo* studies revealed that berberine inhibits the development of colitis-associated colorectal cancer by interfering with inflammatory response-driven EGFR signaling in tumor cell growth [28]. It has been confirmed that EGFR/PI3K/Akt is an important signal pathway in regulating tumor cell proliferation and apoptosis [29]. Once the EGFR combines with ligand, the PI3K/Akt, Ras/Raf/MEK/ERK signal pathways can be activated through cascade reaction [30]. In the PI3K/Akt pathway, multiple growth factors are involved in signal transduction [31], which is considered as the primary pathway for cancer cell survival by researchers globally [32]. EGFR can activate the PI3K/Akt signal pathway by reducing apoptosis and stimulating protein activity [33]. Chun et al. found that in the MDA-MB-231 cells of breast cancer, EGF can stimulate EGFR autophosphorylation and promote cell growth by activating the PI3K/Akt and MAPK signaling pathways [34].

The Akt gene encodes a 56 kDa serine/threonine protein kinase, and locates in the core of PI3K/Akt signaling pathway [35].
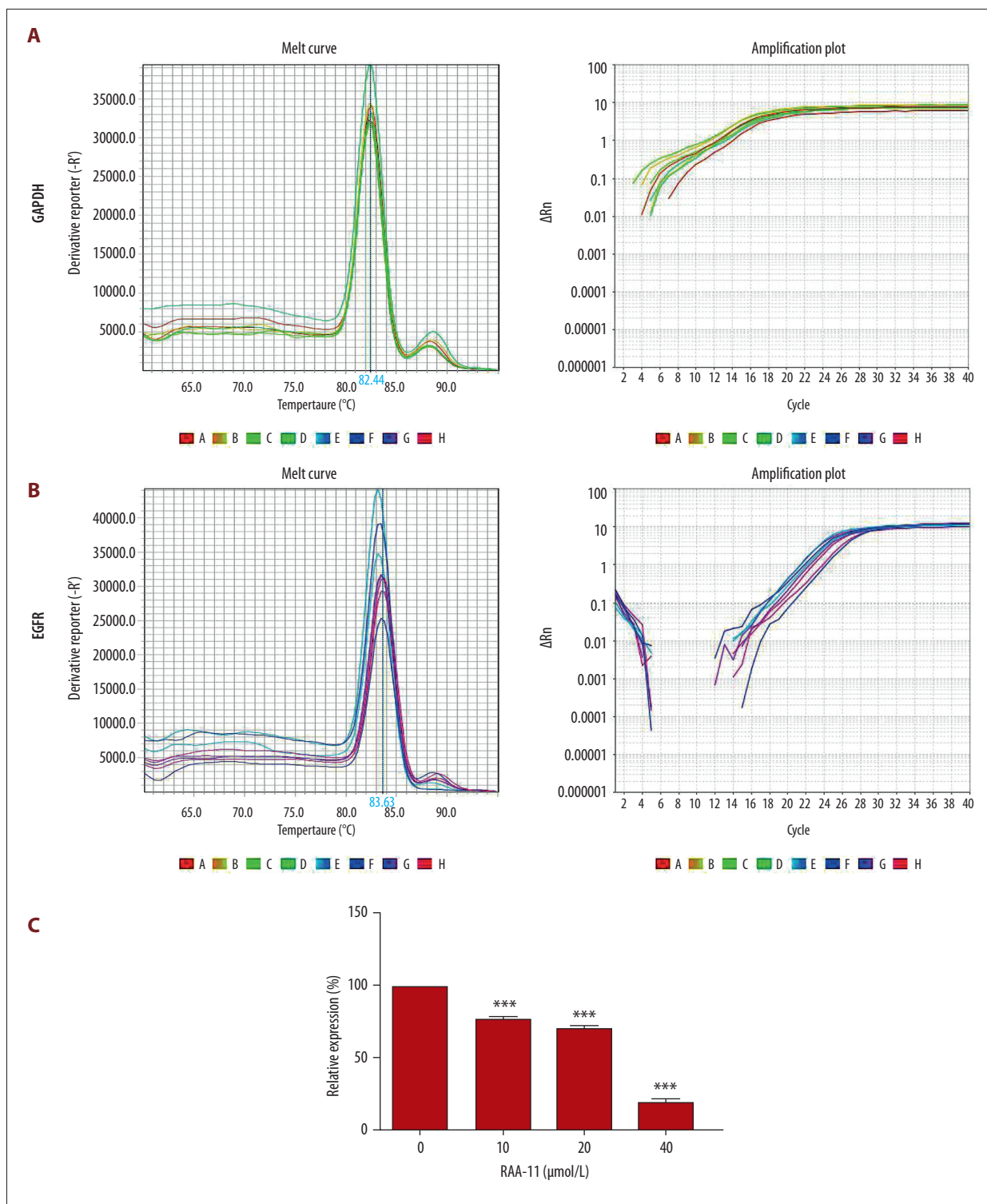
Figure 7. qRT-PCR results show the influence of different concentrations of RAA-11 on the expression level of GAPDH and EGFR mRNA in human gastric cancer cells SGC-7901. (**A**) Melting curve and amplification plot of GAPDH mRNA. (**B**) Melting curve and amplification plot of EGFR mRNA. (**C**) Histogram of EGFR mRNA relative expression. ($\overline{\chi}$±S, n=3), *** P<0.001 versus 0 µmol/L group.
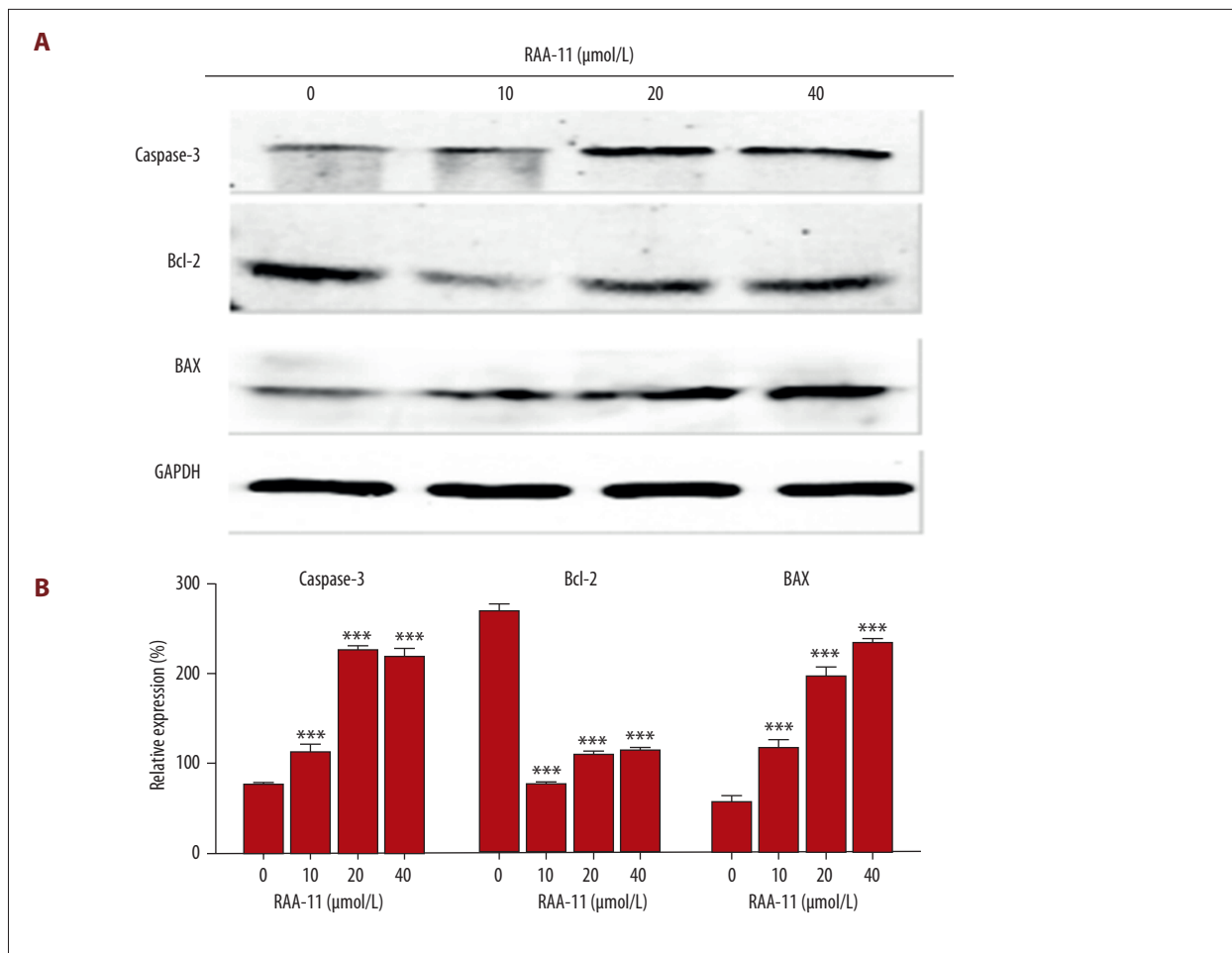
Figure 8. Western blot results. (**A**) Influence of different concentrations of RAA-11 on apoptosis-related proteins caspase-3, Bcl-2, and BAX expression in human gastric cancer cells SGC-7901. (**B**) Histogram of caspase-3, Bcl-2, and BAX apoptosis-related proteins relative expression. The relative expression levels of caspase-3 and BAX proteins were upregulated in a dose-dependent manner, the relative expression level of Bcl-2 in dose groups were significantly reduced compared with 0 μmol/L group. ($\overline{\chi}$±S, n=3), *** P<0.001 versus 0 μmol/L group with the same protein.

The overactivation of the PI3K/Akt signaling pathway can promote cell proliferation by inhibiting the pro-apoptotic pathway, thereby promoting tumor growth [36]. In addition, Akt can regulate the downstream nuclear transcription factor (NF-κB) through mammalian target of rapamycin (mTOR) [37]. NF-κB further regulates a variety of cancer cell effects, including proliferation, apoptosis, metastasis and angiogenesis [38].

As a transcription factor, NF-κB can control tumorigenesis and resist to cancer treatment by regulating a series of genes related to cell proliferation and apoptosis. It can also regulate the apoptosis and cell proliferation, thereby promoting biological behaviors such as tumor angiogenesis, metastasis and invasion. Furthermore, it participates in physiological and pathological processes such as immunity, inflammation and stress response [39,40]. NF-κB is a crucial mediator of inflammatory and immune responses and a number of phytochemicals

that can suppress this immune-regulatory transcription factor are known to have promising anti-inflammatory potential. Liu et al. found that harmine might exert the anti-inflammatory effect by inhibition of the NF-κB signaling pathway [41]. Park et al. thought that inhibiting NF-κB signaling had potential therapeutic applications in cancer and inflammatory diseases [42]. Many studies have suggested that NF-κB is closely related to cancer and plays a key role in the occurrence and development of cancer [43]. Sandner et al. found that in gastric cancer tissue and gastric cancer cells, NF-κB is highly expressed, its activation can not only promote the generation of the chemokine, reactive oxygen species (ROS), prostaglandins, matrix metalloproteinase (MMPs) [44], but it can also alter the phenotype of gastric mucosa cells, involve in cell proliferation, angiogenesis, and cancer cell resistance to apoptosis. Moreover, NF-κB is also related to the prevention, occurrence, development, metastasis, infiltration, treatment and prognosis
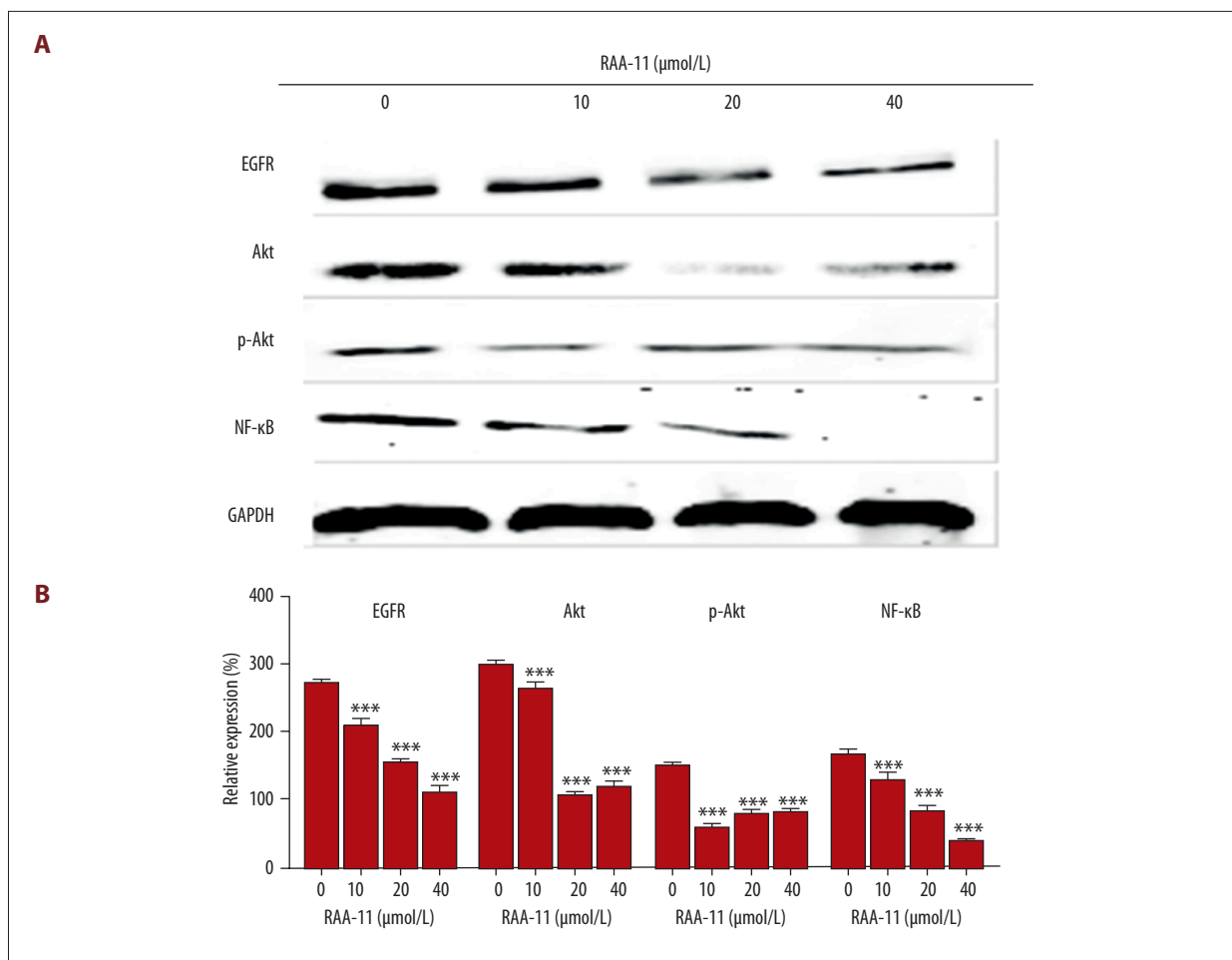
Figure 9. Western blot results. (**A**) Influence of different concentrations of RAA-11 on EGFR, Akt, p-Akt and NF-κB pathway proteins expression in human gastric cancer cells SGC-7901. (**B**) Histogram of EGFR, Akt, p-Akt and NF-κB pathway proteins relative expression. The relative expression levels of EGFR and NF-κB proteins were downregulated in a dose-dependent manner, the relative expression levels of Akt and p-Akt in dose groups were significantly reduced compared with 0 μmol/L group. ($\overline{\chi}$±S, n=3), *** P<0.001 versus 0 μmol/L group with the same protein.

of gastric cancer [45]. Many studies have proven that the abnormal activation of NF-κB signal pathway is closely related to the occurrence and development of various diseases, such as gastric cancer, colon cancer, ulcerative colitis, and helicobacter pylori related gastritis [46–48]. At the same time, our data showed that RAA-11 significantly downregulated the expression of pathway proteins EGFR, Akt, p-Akt, and NF-κB. Therefore, we deem that RAA-11 inhibits the growth and proliferation of SGC-7901 cells and induces apoptosis through the EGFR/Akt/NF-κB pathway.

Conclusions

RAA-11 can effectively inhibit the growth, proliferation and colony forming ability and induce apoptosis of human gastric cancer SGC-7901 cells, whereby the apoptosis mechanism is related to the EGFR/Akt/NF-κB pathway. However, further in-depth studies and preclinical animal studies are needed to assess the exact mechanism of RAA-11 inducing apoptosis of human gastric cancer SGC-7901 cells, so as to draw scientific theoretical basis for the development and application of RAA-11.

Conflict of interest

None.

Indexed in: [Index Medicus/MEDLINE] [EMBASE/Excerpta Medica] [Chemical Abstracts/CAS]

References:

1. Al-Othman S, Haoudi A, Alhomoud S et al: Tackling cancer control in the Gulf Cooperation Council Countries. Lancet Oncol, 2015; 16(5): e246–57

2. Siegel RL, Miller KD, Jemal A: Cancer statistics, 2018. Cancer J Clin, 2018; 68(1): 7–30

3. Almora-Pinedo Y, Arroyo-Acevedo J, Herrera-Calderon O et al: Preventive effect of Oenothera rosea on N-methyl-N-nitrosourea-(NMU) induced gastric cancer in rats. Clin Exp Gastroenterol, 2017; 10: 327–32

4. Tegels JJ, De Maat MF, Hulsewé KW et al: Improving the outcomes in gastric cancer surgery. World J Gastroenterol, 2014; 20(38): 13692–704

5. Sznarkowska A, Kostecka A, Meller K, Bielawski KP: Inhibition of cancer antioxidant defense by natural compounds. Oncotarget, 2016; 8(9): 15996–6016

6. Freitag H, Christen F, Lewens F et al: Inhibition of mTOR's catalytic site by PKI-587 is a promising therapeutic option for gastroenteropancreatic neuroendocrine tumor disease. Neuroendocrinology, 2016; 105(1): 90–104

7. Gutiérrez-Grijalva EP, Picos-Salas MA, Leyva-López N et al: Flavonoids and phenolic acids from oregano: occurrence, biological activity and health benefits. Plants (Basel), 2018; 7(1): 2

8. Han S, Yang S, Cai Z et al: Anti-Warburg effect of rosmarinic acid via miR-155 in gastric cancer cells. Drug Des Devel Ther, 2015; 9: 2695–703

9. Kim GD, Park YS, Jin YH, Park CS: Production and applications of rosmarinic acid and structurally related compounds. Appl Microbiol Biotechnol, 2015; 99(5): 2083–92

10. Rocha J, Eduardo-Figueira M, Barateiro A et al: Anti-inflammatory effect of rosmarinic acid and an extract of rosmarinus officinalis in rat models of local and systemic inflammation. Basic Clin Pharmacol Toxicol, 2015; 116(5): 398–413

11. Zhu F, Asada T, Sato A et al: Rosmarinic acid extract for antioxidant, antiallergic, and α-glucosidase inhibitory activities, isolated by supramolecular technique and solvent extraction from Perilla leaves. J Agric Food Chem, 2014; 62(4): 885–92

12. Ji CF, Ji YB: Apoptosis of human gastric cancer SGC-7901 cells induced by podophyllotoxin. Exp Ther Med, 2014; 7(5): 1317–22

13. Supreeth M, Chandrashekar MA, Sachin N, Raju NS: Effect of chlorpyrifos on soil microbial diversity and its biotransformation by Streptomyces sp. HP-11. 3 Biotech, 2016; 6(2): 147

14. Hu S, Li X, Xu R et al: The synergistic effect of resveratrol in combination with cisplatin on apoptosis via modulating autophagy in A549 cells. Acta Biochim Biophys Sin (Shanghai), 2016; 48(6): 528–35

15. Xu S, Shu P, Zou S et al: NFATc1 is a tumor suppressor in hepatocellular carcinoma and induces tumor cell apoptosis by activating the FasL-mediated extrinsic signaling pathway. Cancer Med, 2018; 7(9): 4701–17

16. Skrt M, Benedik E, Podlipnik C, Ulrih NP: Interactions of different polyphenols with bovine serum albumin using fluorescence quenching and molecular docking. Food Chem, 2012; 135(4): 2418–24

17. Habtemariam S: Molecular pharmacology of rosmarinic and salvianolic acids: Potential seeds for Alzheimer's and vascular dementia drugs. Int J Mol Sci, 2018; 19(2): pii: E458

18. Neves JA, Neves JA, Oliveira RCM: Pharmacological and biotechnological advances with Rosmarinus officinalis L. Expert Opin Ther Pat, 2018; 28(5): 399–413

19. Bauer N, Vuković R, Likić S, Jelaska S: Potential of different Coleus blumei tissues for rosmarinic acid production. Food Technol Biotechnol, 2015; 53(1): 3–10

20. Wang X, He Z, Liu H et al: Neutrophil necroptosis is triggered by ligation of adhesion molecules following GM-CSF priming. J Immunol, 2016; 197(10): 4090–100

21. Zheng Y, Wu Y, Chen X et al: Chinese propolis exerts anti-proliferation effects in human melanoma cells by targeting NLRP1 inflammatory pathway, inducing apoptosis, cell cycle arrest, and autophagy. Nutrients, 2018; 10(9): pii: E1170

22. Li SX, Cui N, Zhang CL et al: Effect of subchronic exposure to acrylamide induced on the expression of bcl-2, bax and caspase-3 in the rat nervous system. Toxicology, 2006; 217(1): 46–53

23. Brentnall M, Rodriguez-Menocal L, De Guevara RL et al: Caspase-9, caspase-3 and caspase-7 have distinct roles during intrinsic apoptosis. BMC Cell Biol, 2013; 14: 32

24. Yin Z, Qi H, Liu L, Jin Z: The optimal regulation mode of Bcl-2 apoptotic switch revealed by bistability analysis. Biosystems, 2017; 162: 44–52

25. Beaumont TE, Shekhar TM, Kaur L et al: Yeast techniques for modeling drugs targeting Bcl-2 and caspase family members. Cell Death Dis, 2013; 4(5): e619

26. Yue J, Lv D, Wang C et al: Epigenetic silencing of miR-483-3p promotes acquired gefitinib resistance and EMT in EGFR-mutant NSCLC by targeting integrin β3. Oncogene, 2018; 37(31): 4300–12

27. Mu Z, Klinowska T, Dong X et al: AZD8931, an equipotent, reversible inhibitor of signaling by epidermal growth factor receptor (EGFR), HER2, and HER3: Preclinical activity in HER2 non-amplified inflammatory breast cancer models. J Exp Clin Cancer Res, 2014; 33(1): 47

28. Li D, Zhang Y, Liu K et al: Berberine inhibits colitis-associated tumorigenesis via suppressing inflammatory responses and the consequent EGFR signaling-involved tumor cell growth. Lab Invest, 2017; 97(11): 1343–53

29. Zhang Y, Xiang C, Wang Y et al: LncRNA LINC00152 knockdown had effects to suppress biological activity of lung cancer via EGFR/PI3K/AKT pathway. Biomed Pharmacother, 2017; 94: 644–51

30. Schnidar H, Eberl M, Klingler S et al: Epidermal growth factor receptor signaling synergizes with Hedgehog/GLI in oncogenic transformation via activation of the MEK/ERK/JUN pathway. Cancer Res, 2009; 69(4): 1284–92

31. Luan M, Li N, Pan W et al: Simultaneous detection of multiple targets involved in the PI3K/AKT pathway for investigating cellular migration and invasion with a multicolor fluorescent nanoprobe. Chem Commun (Camb), 2016; 53(2): 356–59

32. Huang J, Zhang L, Greshock J et al: Frequent genetic abnormalities of the PI3K/AKT pathway in primary ovarian cancer predict patient outcome. Genes Chromosomes Cancer, 2011; 50(8): 606–18

33. Su JC, Lin KL, Chien CM et al: Naphtho [1,2-b]furan-4,5-dione inactivates EGFR and PI3K/Akt signaling pathways in human lung adenocarcinoma A549 cells. Life Sci, 2010; 86(5–6): 207–13

34. Chun J, Kim YS: Platycodin D inhibits migration, invasion, and growth of MDA-MB-231 human breast cancer cells via suppression of EGFR-mediated Akt and MAPK pathways. Chem Biol Interact, 2013; 205(3): 212–21

35. Cheng JQ, Godwin AK, Bellacosa A et al: AKT2, a putative oncogene encoding a member of a subfamily of protein-serine/threonine kinases, is amplified in human ovarian carcinomas. Proc Natl Acad Sci USA, 1992; 89(19): 9267–71

36. Byun HJ, Kim BR, Yoo R et al: sMEK1 enhances gemcitabine anti-cancer activity through inhibition of phosphorylation of Akt/mTOR. Apoptosis, 2012; 17(10): 1095–103

37. Subramanian C, Grogan PT, Opipari VP et al: Novel natural withanolides induce apoptosis and inhibit migration of neuroblastoma cells through down regulation of N-myc and suppression of Akt/mTOR/NF-κB activation. Oncotarget, 2018; 9(18): 14509–23

38. Serwe A, Rudolph K, Anke T, Erkel G: Inhibition of TGF-β signaling, vasculogenic mimicry and proinflammatory gene expression by isoxanthohumol. Invest New Drugs, 2012; 30(3) 898–915

39. Ma J, Gao Q, Zeng S, Shen H: Knockdown of NDRG1 promote epithelial-mesenchymal transition of colorectal cancer via NF-κB signaling. J Surg Oncol, 2016; 114(4): 520–27

40. Aggarwal BB, Sung B: NF-κB in cancer: A matter of life and death. Cancer Discov, 2011; 1(6): 469–71

41. Liu X, Li M, Tan S et al: Harmine is an inflammatory inhibitor through the suppression of NF-κB signaling. Biochem Biophys Res Commun, 2017; 489(3): 332–38

42. Park MH, Hong JT: Roles of NF-κB in cancer and inflammatory diseases and their Therapeutic approaches. Cells, 2016; 5(2): 15

43. Zhao XD, Lu YY, Guo H et al: MicroRNA-7/NF-κB signaling regulatory feedback circuit regulates gastric carcinogenesis. J Cell Biol, 2015; 210(4): 613–27

44. Sandner A, Illert J, Koitzsch S et al: Reflux induces DNA strand breaks and expression changes of MMP1+9+14 in a human miniorgan culture model. Exp Cell Res, 2013; 319(19): 2905–15

45. Shibata W, Takaishi S, Muthupalani S et al: Conditional deletion of IkappaB-kinase-beta accelerates helicobacter-dependent gastric apoptosis, proliferation, and preneoplasia. Gastroenterology, 2009; 138(3): 1022–34

46. Qin W, Li C, Zheng W et al: Inhibition of autophagy promotes metastasis and glycolysis by inducing ROS in gastric cancer cells. Oncotarget, 2015; 6(37): 39839–54

47. Kim EJ, Kwon KA, Lee YE et al: Korean Red Ginseng extract reduces hypoxia-induced epithelial-mesenchymal transition by repressing NF-κB and ERK1/2 pathways in colon cancer. J Ginseng Res, 2017; 42(3): 288–97

48. Peng LS, Zhuang Y, Li WH et al: Elevated interleukin-32 expression is associated with Helicobacter pylori-related gastritis. PLoS One, 2014; 9(3): e88270